Analysis of evaporation of high-salinity phreatic water at a burial depth of 0 m in an arid area

JIA Rui-liang [1], ZHOU Jin-long [1,2,3*], LI Qiao [1], LI Yang [1]

[1] College of Water Conservancy and Civil Engineering, Xinjiang Agricultural University, Urumqi 830052, China.
[2] Institute of Hydrogeology and Environmental Geology, Chinese Academy of Geological Sciences, Shijiazhuang 050061, China.
[3] School of Environmental Science, China University of Geosciences, Wuhan 430074, China.

Abstract: High-salinity phreatic water refers to which with total dissolved solids (TDS)>30 g/L. Previous studies have shown that high salinity phreatic water evaporation is different at different depths. High salinity phreatic water evaporation under 0 m depth is the basis of the high salinity phreatic water evaporation studies. In this study, evaporation of high-salinity phreatic water at a burial depth of 0 m in arid area was investigated. New insights were gained on evaporation mechanisms via experiments conducted on high-salinity phreatic water with TDS of 100 g/L at 0 m at the study site at Changji Groundwater Balance Experiment Site, Xinjiang Uygur Autonomous Region in China, where the lithology of the vadose (unsaturated zone) was silty clay. Comparison was made on the data of high-salinity phreatic water evaporation, water surface evaporation ($E_{\Phi 20}$) and meteorological data obtained in two complete hydrological years from April 1, 2012 to March 31, 2014. The experiments demonstrated that when the lithology of the vadose zone is silty clay, the burial depth is 0 m and the TDS is 100 g/L, intra-annual variation of phreatic water evaporation is the opposite to the variation of atmospheric evaporation $E_{\Phi 20}$ and air temperature. The salt crust formed by the evaporation of high-salinity phreatic water has a strong inhibitory effect on phreatic water evaporation. Large volumes of precipitation can reduce such an inhibitory effect. During freezing periods, surface snow cover can promote the evaporation of high-salinity phreatic water at 0 m; the thicker the snow cover, the more apparent this effect is.

Keywords: Arid area; High-salinity phreatic water; Phreatic water evaporation at the burial depth of 0 m; Water evaporation

Phreatic water evaporation is the process by which phreatic water flows into the vadose zone, where it evaporates from the soil and is transpired by plants (LEI Zhi-dong *et al*. 1999). Phreatic water evaporation describes a major natural transformation of shallow groundwater into soil water and atmospheric water. It is a crucial component of transformation between the "four waters", namely atmospheric water, surface water, soil water and ground water (ZHOU Jin-long *et al*. 2002). As a major discharge component in shallow groundwater areas, phreatic water evaporation needs to be accurately calculated so as to correctly evaluate groundwater resources. For regions lacking field monitoring data, the main method to calculate phreatic water evaporation involves using empirical formulas. Among many empirical formulas, the most commonly used are Aver'yanov's phreatic evaporation equations (ZHOU Jin-long *et al*. 2002), Lei's formula (HU Shu-jun *et al*. 2005), Ye's exponential equation (FU Qiu-ping *et al*. 2007) and various power functions fitted for different regions (XING Xu-guang *et al*. 2013). All these equations employ E_0 as the term describing phreatic water evaporation intensity at the burial depth of 0 m. Existing studies show that when the lithology of the vadose zone is fine sand or gravel, E_0 is approximately equal to the intensity of atmospheric evaporation, and therefore can be substituted for water surface evaporation. When the lithology of the vadose zone is not fine sand or gravel, the value of E_0 is not equal to the intensity of water surface evaporation, and therefore should

*Corresponding author. Email: zjzhoujl@163.com

be taken as the intensity corresponding to 0 m burial depth (HU Shu-jun *et al*. 2005; FU Qiu-ping *et al*. 2007; XING Xu-guang *et al*. 2013). In studies on phreatic water evaporation at burial depths of 0 m, only the influence of the lithology in the vadose zone is considered in relation to phreatic water evaporation intensity, but not the possible influence of the phreatic water salinity.

This last omission is important, given that in the arid regions of Hexi Corridor, Junggar Basin, Tarim Basin, Turpan Basin and Qaidam Basin, brine water formed by salinization and concentration is very common. Usually, average salinity levels are 3-10 g/L, and sometimes greater than 50 g/L. The salinity of brine water in Hexi Corridor can reach 100 g/L. In Qaidam Basin, phreatic water salinity can be as high as 300 g/L (Editorial Board of the Physical Geography of China of the Chinese Academy of Sciences, 1981). When high-salinity phreatic water is located near salt lakes, or around salt marshes, or in saline land in shallow groundwater regions located downstream of reservoirs, the influence of phreatic water salinity on phreatic water evaporation cannot be ignored (LI Xian-wen *et al*. 2012). For regions with high-salinity phreatic water, the lithology of the vadose zone is usually silty clay or fine sand. Compared with phreatic water evaporation in other areas, the evaporation of high-salinity phreatic water in arid regions is quite different in terms of the capillary water height, critical depth of salt, composition of total water soil water potential, unsaturated hydraulic conductivity, and soil moisture characteristics (LI Xian-wen *et al*. 2012). Previous studies have shown that high salinity phreatic water evaporation is different at different depths (JIA Rui-liang *et al*. 2015). All these factors will affect the rate of phreatic water evaporation. At a burial depth of 0 m for the same region, high-salinity phreatic water evaporation may be also different, and thus the value of E_0 should be selected with caution.

1 Materials and methods

A Lysimeter was used to collect the data on high-salinity phreatic water evaporation in 2 hydrological years at two locations with a typical arid climate: Changji Groundwater Balance Experiment Site from Bureau of Geology and Mineral Resources Development of Xinjiang. The dynamic relationship between high-salinity phreatic water evaporation at the burial depth of 0 m and atmospheric evaporation capability was analyzed. On this basis, the rules and mechanism of high-salinity phreatic water evaporation at the burial depth of 0 m were identified. Our study provides data for understanding the mechanism of high-salinity phreatic water evaporation in arid areas. Using the method proposed in this article, we can more accurately calculate the evaporation of high-salinity phreatic water, the evaporation of phreatic water in salty land in downstream from reservoirs, the water consumption of salt marshes and evaporation of phreatic water along lake shores.

1.1 Study area

Changji Groundwater Balance Experiment Site is located on the western edge of an alluvial-pluvial fan of the Toutun River at the northern piedmont of Tianshan Mountains (87°17′51″E, 44°02′19″N). The experimental site was defined as an area 1.5×10^4 m^2 with an elevation of 538 m and 4.7 km distant from the Toutun River riverbed. The terrain was open, flat and distant from high-rise buildings. The experiment site experiences climate typical of the inland region, with an annual mean air temperature of 7.1 °C and an annual mean precipitation of 196.9 mm falling predominantly between April and August. Annual mean evaporation is 1 819.3 mm ($E_{\Phi 20}$) and occurs predominantly between April and October. Annual mean wind speed is 1.1 m/s and the soil freezing period of soil is 5 months between November and March. The depth of the permafrost zone is generally 80-130 cm. The geographical and geomorphological conditions of the experimental station are representative and typical of the agricultural area in the south margin of the Junggar Basin at the Northern Piedmont of Tianshan Mountains.

1.2 Experimental design

A lysimeter used to collect the data of phreatic water evaporation was composed of a soil sample collector, water supply system and a monitoring device. The soil sample collector was a barrel with

a cross sectional area of 4.0 m^2. The results of particle-size analysis are shown in Table 1. The soil samples used were disturbed silty clay which were compacted by stratified filling at the dry density of 1.58 g/cm^3 in 1989, and were since compacted once every 20 cm filled. Water saturation readings were performed once every 60 cm filled to strength the compactness. At the bottom of the soil was 30 cm thick gravel filtering layer. The top was bard land, which was leveled to the ground surface level. The water supply system consisted of a modified Markov bottle (constant eluent bottle). The burial depth of the phreatic water in the lysimeter was controlled at 0 m. Changes to the water level in the Markov bottle were observed to determine phreatic water evaporation. C1-Na type water is the most common hydrochemical type of high-salinity phreatic water in arid areas. In our experiments, 100 g/L phreatic water was prepared using industrial salt (NaCl). The phreatic water evaporation was denoted as E_0 (100) (lithology of the vadose zone - silty clay; burial depth of phreatic water - 0 m; salinity of phreatic water - 100 g/L). Atmospheric evaporation capability means that under water-sufficient conditions, water evaporated from the unit amount of water into the atmosphere at unit time. Atmospheric evaporation capability was determined using water surface evaporation $E_{\Phi 20}$ in an evaporator with a diameter of 20 cm and containing fresh water.

Table 1 Results of particle-size analysis of soil samples

	Soil particle composition (%)			
Silty clay	2-0.05 mm	0.05-0.005 mm	0.005-0.002 mm	<0.002 mm
	21.0	45.0	17.3	16.7

The experimental monitoring period was from September 1, 2011 to April 30, 2014. The phreatic water evaporation E_0 (100) was recorded using lysimeter, and water surface evaporation $E_{\Phi 20}$ was observed in a lysimeter at 20:00 Beijing time. Before the experiment, the soil sample collector was only used for phreatic water observation of fresh water. Considering the high-salinity water distribution tend to stability in the soil and the comparability in time for high-salinity phreatic water, the monitoring period was from April 1 2012 to March 31 2014, totalling 730 d, which belongs to the test period and namely two complete hydrological years. The data obtained over two hydrological years were pooled for analysis.

2 Results and discussion

Precipitation and air temperature data during the monitoring period were derived from meteorological observation data at Changji Station. For E_0 (100), $E_{\Phi 20}$ and meteorological observation data (Table 2).

Table 2 E_0 (100), $E_{\Phi 20}$ and meteorological observation data

Time (year. month)	E_0(100)	$E_{\Phi 20}$	Precipitation	Air temperature	Ground temperature	Maximum snow thickness
	mm	mm	mm	℃	℃	cm
2012.4	57.9	231.5	4.5	16.2	19.4	
2012.5	36.7	311.1	0.0	21.6	26.0	
2012.6	40.2	346.0	14.3	24.1	29.4	
2012.7	30.2	343.6	7.5	26.6	32.8	
2012.8	28.2	338.0	16.5	24.8	29.7	
2012.9	22.8	206.2	11.9	18.5	20.9	
2012.10	46.8	119.1	11.8	9.0	9.0	
2012.11	109.0	30.8	30.4	-4.1	-3.8	
2012.12	60.3	8.9	24.4	-16.2	-22.2	31.0
2013.1	113.2	7.3	5.9	-15.1	-19.3	32.7

Table 2 (Continued)

2013.2	305.8	12.9	5.1	-11.7	-22.1	36.3
2013.3	149.9	88.4	6.2	5.0	4.4	27.0
2013.4	43.8	188.3	26.7	14.1	17.9	
2013.5	30.2	264.5	12.1	19.0	25.6	
2013.6	29.0	308.5	18.6	24.4	30.2	
2013.7	29.0	350.5	8.8	26.2	32.2	
2013.8	26.1	300.6	16.3	24.2	28.7	
2013.9	22.8	203.5	6.1	18.3	20.5	
2013.10	27.0	116.7	8.5	15.4	10.8	
2013.11	26.8	18.5	19.8	0.0	-1.2	
2013.12	24.4	5.5	8.1	-6.8	-6.7	5.3
2014.1	80.2	7.3	3.5	-14.1	-13.8	9.3
2014.2	142.2	14.3	20.0	-14.3	-13.2	22.0
2014.3	24.5	63.8	21.0	0.5	0.3	23.0

Note: Ground temperature is the temperature of bare land.

2.1 Influence of atmospheric evaporation capability $E_{\Phi 20}$ on E_0 (100)

The variation in phreatic evaporation E_0 (100) is directly opposite to that of atmospheric evaporation capability $E_{\Phi 20}$ (Fig. 1). From early March to middle October every year, the atmospheric evaporation capability first increased and then decreased, with the peak occurring around July. In contrast, evaporation of high-salinity phreatic water at the burial depth of 0 m first decreased, stabilised somewhat and then gradually increased. More specifically for high-salinity phreatic water, from March to April, rates of evaporation decreased over time, reaching a considerably small value after April and varying only slightly in the months following. The rate of evaporation gradually increased from September to October. While atmospheric evaporation capability was at its maximum, the evaporation of high-salinity phreatic water at the burial depth of 0 m fell to a minimum. From mid-October in 2012 and 2013 to early March of the following year, atmospheric evaporation capability first decreased and then increased, reaching the trough value around January. However, E_0 (100) first increased first and then decreased, with the peak appearing in about February.

In regards to the pattern we see in non-freezing periods, the evaporation of high-salinity phreatic water at the burial depth of 0 m contradicts previous observations that the relationship between the intensity of atmospheric evaporation and that of phreatic water evaporation at burial depth of 0 m are consistent (HU Shu-jun *et al*. 2005). One reason for the alternative observations we see in our study is that at the burial depth of 0 m, evaporation is essentially aligned with water surface evaporation. However, due to the high salinity of phreatic water, the crystallization of soil NaCl causes the soil salt content to increase. Na^+ has an extremely high water adsorption, therefore high Na^+ content will enhance inhibitory effects on evaporation rates. The occurrence of phreatic water evaporation facilitates the retention of salt in surface soil. The salt accumulation on the surface thereby lowers the surface evaporation rate. As a result, a layer of salt crust is formed (Fig. 2), and a two-layered soil surface structure appears. Salt crust has a poor permeability. As the main component of salt crust, Na^+ has a strong water adsorption that blocks water evaporation from the underlying layer. Thus, the evaporation of phreatic water is reduced. As evaporation continues, the salt crust constantly increases in thickness, producing a more apparent inhibitory effect on phreatic water evaporation (ZHANG Jiang-guo *et al*. 2010). This process is reflected in our results, such that during the early months of the non-freezing period, evaporation decreased gradually, but after April a stable layer of salt crust has formed, causing the rate of phreatic water evaporation to remain at a very small value.

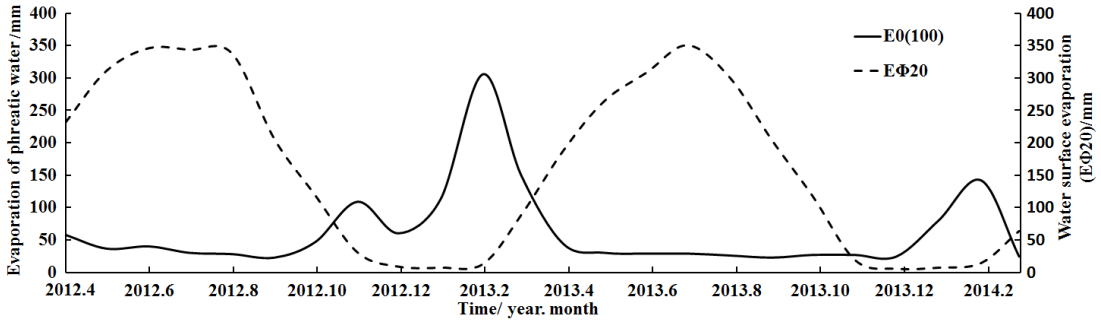

Fig. 1 Trends of E_0 (100) and $E_{\Phi 20}$ over the study period

Fig. 2 Salt crust on the surface of the lysimeter in August 2013

The freezing period was between November and March of the following year during which time solar radiation attenuated, air temperature fell below zero, and atmospheric evaporation capability declined. At this time, snowfall was heavy in the study area, with the soil usually entirely covered between December and March. Snow cover on soil not only prevents the loss of heat from the underground, but also delays the influence of climate on the thermal status of soil (MA Hong and HU Ru-ji, 1995). As the concentration of NaCl increased in solution, both the freezing point of solution and the freezing speed decreased, when the salinity of phreatic water is 100 g/L, its freezing temperature is approximately -6 °C (WU Feng-chun and YANG Yu-ying, 1991). Therefore we attribute the increased evaporation during freezing periods to the fact that snow cover can induce higher ground temperature than the external air temperature. Meanwhile, the high salinity of phreatic water causes the freezing temperature of groundwater to decrease. Thus, the phreatic water under snow cover in freezing period (E_0 (100)) is frozen or partially frozen.

The precipitation in November at the beginning of the freezing period is mainly in the form of rain (Table 2). The precipitation of this month is higher than that of the several months preceding or following. Although some rainfall does not initially destroy the soil surface salt crust, it can be eroded if precipitation is high enough. Because the snow cover is in direct contact with the salt crust, the thawing of snow at the beginning of the freezing period moistens the soil and dissolves the salt crust. The combination of these mechanisms eventually causes a reduction in the inhibitory effect of the salt crust on phreatic water evaporation. When the burial depth is 0 m, the phreatic water is in direct contact with the snow, and there is no salt crust to block the transport of phreatic water. High salinity leads to a high solute potential in the soil, which propels the transport of high-salinity phreatic water to low-salinity snow, thus finally forming an ice-snow mixture. The snow is loose in texture allowing it to accommodate more water. Therefore, the phreatic water evaporation in the freezing period is far higher than that in the non-freezing period.

2.2 Influence of temperature on E_0 (100)

Fig. 3 illustrates that the variation process lines of air temperature and ground temperature are virtually consistent. Moreover, fluctuations in $E_{\Phi 20}$ are also consistent with those of air temperature

and ground temperature. This indicates that temperature is an important factor determining the atmospheric evaporation capability. As temperature increases, the atmospheric evaporation capability is improved accordingly. It also follows that as temperature decreases, the atmospheric evaporation capability declines. When air temperature reaches a peak in July, $E_{\Phi 20}$ also reaches a peak. During the freezing period when air temperature fell below 0 °C, $E_{\Phi 20}$ was small and relatively stable during the entire freezing period, with a mean of only 13.2 mm/month. Fig. 3 also illustrates that trends in air temperature and ground temperature are the opposite to those of E_0 (100). As we have discussed above, powerful evaporation during the non-freezing period causes the formation of salt crust on the soil surface, which blocks the evaporation of phreatic water. On the other hand, due to the protective effect of snow cover during the freezing period, the temperature under the snow cover is higher than the air temperature, thereby promoting the transport of phreatic water into the snow cover, and enhancing phreatic water evaporation.

2.3 Influence of precipitation on E_0 (100)

Precipitation is not significantly correlated to atmospheric evaporation capability $E_{\Phi 20}$, but in some respects is related to E_0 (100) (Fig. 4). For example, in November 2012 a small peak of E_0 (100) occurred, but this phenomenon did not recur in the same month of 2013. Precipitation trends illustrated in Fig. 4, show maximum precipitation was reached in November 2012. The meteorological observation data (Table 2) indicate that in November 2012 the main form of precipitation was rain. In this case, we can then assume that the salt crust on the soil surface in the lysimeter to be washed away by the rain. Hence the phreatic water evaporation was larger than that of the same period in which less precipitation occurred. Our assumptions are justified in Fig. 4, which clearly shows the trends of phreatic water evaporation and precipitation were consistent in November 2012, but not in November 2013. Without sufficient precipitation in November 2013, the salt crust would not have been eroded. Indeed, less rainfall only results in more severe salt conditions and a thicker salt crust, and hence a stronger inhibitory effect on phreatic water evaporation (SHAO Ming-an *et al*. 2006). It is easy to see that on bare land, the formation of salt crusts on the soil surface is an important factor in blocking phreatic water evaporation (ZHANG Jiang-guo *et al*. 2010). Greater rainfall events destroy the salt crust formed on the soil surface, leading to temporary rise of phreatic water evaporation.

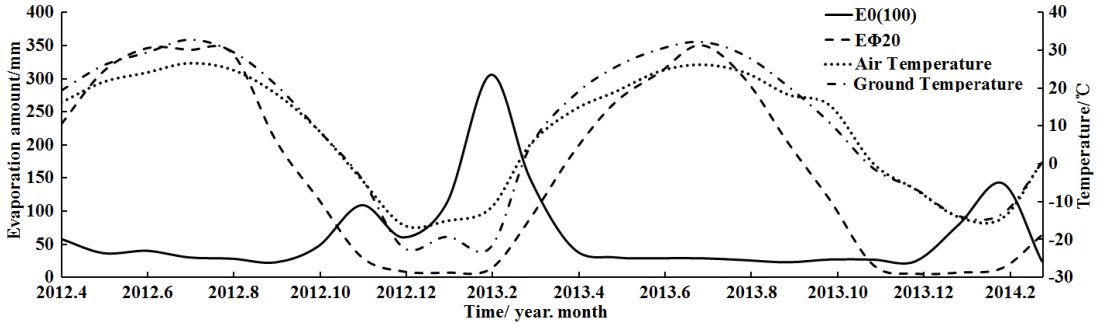

Fig. 3 Process lines of E_0 (100), $E_{\Phi 20}$ and temperature

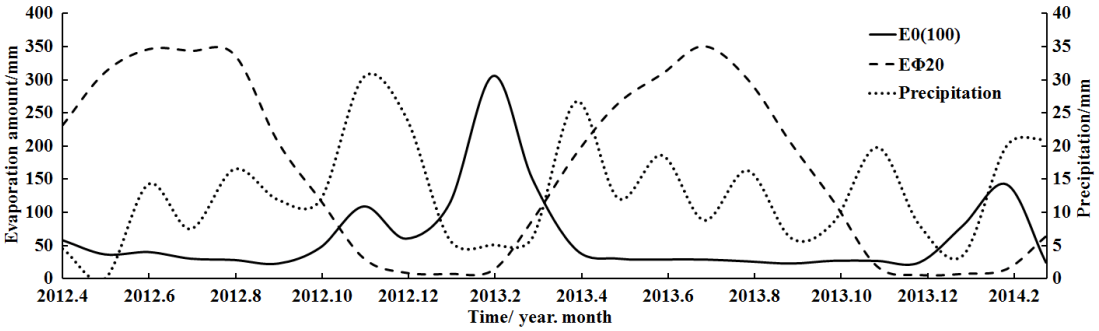

Fig. 4 Process lines of E_0 (100), $E_{\Phi 20}$ and precipitation

2.4 Effect of snow thickness on E_0 (100)

Phreatic water evaporation during the freezing period of the October 2012 to March 2013 was obviously higher than that of October 2014 to March 2014. In Table 2, the maximum snow thickness during each month of the freezing period in October 2012 to March 2013 was always larger than that of October 2014 to March 2014. The mean snow thickness during the October 2012 to March 2013 (freezing period) was 33.3 cm, with a maximum of 36.3 cm. In October 2014 to March 2014, the mean snow thickness was 12.2 cm, and the maximum was only 22.0 cm. As seen in Table 2, the snow also accumulated on the ground in March every year. But when the air temperature rose over 0 °C, the snow rapidly thawed. Observation data notes that each year there is virtually no snow accumulation on the ground after the middle of March. Table 2 shows that snow thickness during the freezing period increased gradually and peaking in February. Corresponding with the snow accumulation data in Table 2, Fig. 1 illustrates that phreatic water evaporation began to increase in December each year of the study period, reaching a peak in February. This analysis demonstrates that the existence of snow cover in the freezing period caused the increase of evaporation of high-salinity phreatic water, which has been shown to be directly proportionate to snow cover thickness (MA Hong and HU Ru-ji, 1995). As we have stated, snow cover has a heat insulation effect on the underlying soil layer, thereby increasing the flow of phreatic water into the snow, where evaporation occurs. The thicker the snow cover, the greater the heat insulation effect on the underlying soil layer, and it follows that as more evaporated water accumulates in the snow, the snow thickness increases. This snow insulation effect explains the greater evaporation rates of high-salinity phreatic water. Consequently, the evaporation of high-salinity phreatic water in the freezing period of October 2012 to March 2013 was higher than that of October 2013 to March 2014. The peak of phreatic water evaporation occurred in February every year.

3 Conclusions

In our study, we compared phreatic water evaporation in a lysimeter (silty clay, burial depth of 0 m, salinity 100 g/L) to atmospheric evaporation capability and meteorological data of the same period. The following conclusions were made:

(1) When the lithology of the vadose zone was silty clay, burial depth was 0 m and salinity of phreatic water was 100 g/L, the intra-annual variation of phreatic water evaporation was directly opposite to trends in atmospheric evaporation capability $E_{\Phi 20}$ and local air temperature.

(2) During non-freezing periods at a burial depth of 0 m, evaporation caused the salt in high-salinity phreatic water to accumulate on the surface, which strongly inhibited the subsequent evaporation of phreatic water. Moreover, large rainfall events can destroy the salt crust, thus producing an inhibitory effect on phreatic water evaporation.

(3) During the freezing periods, snow cover significantly promoted the evaporation of high-salinity phreatic water at 0 m. The thicker the snow cover, the more pronounced this effect is.

Our study of phreatic water evaporation at 0 m is critical for calculating phreatic water evaporation as a whole. As we have discussed, evaporation of high-salinity phreatic water and that of fresh water at a burial depth of 0 m differ greatly. Furthermore, temperature potential in the non-freezing period also had a negligibly small influence on the movement of water in soil. However, temperature potential is a leading factor for water movement in soil during the freezing period (SHAO Ming-an, 2006). This phenomenon was quite unexpected, and provides ground for further investigation. One leading question centers around the relationship between evaporation of high-salinity phreatic water, ground temperature in the lysimeter and the temperature of the lower, middle and surface of snow cover. A second line of inquiry demands whether during the freezing period when snow cover exists, how the evaporated phreatic water flows into the accumulated snow. All these questions deserve more thorough research.

Acknowledgements

The research was sponsored by National

Natural Science Foundation of China (51069016) and Foundation of Key Disciplines in Hydrology and Water Resources of Xinjiang Uygur Autonomous Region (xjswszyzdxk20101202).

References

Editorial Board of the Physical Geography of China of the Chinese Academy of Sciences. 1981. The physical geography of China-groundwater. Beijing: Science Press, 69, 72-75.

FU Qiu-ping, ZHANG Liang-hui, WANG Quan-jiu, *et al*. 2007. Impact of E_o value on calculation accuracy of phreatic evaporation empirical formulae. Arid Land Geography, 30(6):820-825.

JIA Rui-liang, ZHOU Jin-long, GAO Ye-xin, *et al*. 2015. Preliminary analysis on evaporation rules of high-salinity phreatic water in arid area. Advances in Water Science, 26(1):44-50.

HU Shu-jun, SONG Yu-dong, TIAN Chang-yan, *et al*. 2005. Relationship between water surface evaporation and phreatic water evaporation when phreatic water buried depth is zero for different soil in Tarim River basin. Transactions of the Chinese Society Agricultural Engineering, 21(S1):80-83.

LEI Zhi-dong, SHANG Song-hao, YANG Shi-xiu, *et al*. 1999. Simulation on phreatic evaporation during soil freezing. Journal of Hydraulic Engineering, 30(6):6-10.

LI Xian-wen, ZHOU Jin-long, JIN Meng-gui, *et al*. 2012. Experiment on evaporation of high-TDS phreatic water in arid area. Journal of Water Resources & Water Engineering, 23(5): 6-10.

LI Xian-wen, ZHOU Jin-long, JIN Meng-gui, *et al*. 2012. Soil-water characteristic curves of high-TDS and suitability of fitting models. Transactions of the Chinese Society Agricultural Engineering, 28(13): 135-141.

MA Hong, HU Ru-ji. 1995. Effects of snow cover on thermal regime of frozen soil. Arid Land Geography, 18(4):23-27.

SHAO Ming-an, WANG Quan-jiu, HUANG Ming-fu. 2006. Soil physics. Beijing: Higher Education Press, 63-64.

WU Feng-chun, YANG Yu-ying. 1991. The discussiones on the freezing-point depression. Journal of Inner Mongolia Teachers University (Natural Science Edition), 8(3):55-58.

XING Xu-guang, SHI Wen-juan, WANG Quan-jiu. 2013. Discussion on E_0 value in common groundwater evaporation empirical models. Agricultural Research in the Arid Areas, 31(4):57-60.

ZHANG Jiang-guo, SUN Shu-guo, XU Xin-wen, *et al*. 2010. Chemical characteristics and its effect on soil evaporation of soil salt crusts in the Tarim desert highway shelterbelts. Journal of Arid Land Resources and Environment, 24(4):174-179.

ZHANG Jiang-guo, XU Xin-wen, LEI Jia-qiang, *et al*. 2010. Effects of salt crust on soil evaporation condition with saline-water drip-irrigation in extreme arid region. Transactions of the Chinese Society Agricultural Engineering, 26(9):34-39.

ZHOU Jin-long, *et al*. 2002. Experiment on the transforming relationship of atmospheric precipitation, irrigation water and soil water and groundwater water in plain area of Xinjiang. Urumqi: Xinjiang Sci-Tech and Public Health Press, 57-65.